Vol 2 (2) (2021)

MCA

Measurement, control and automation

Website: https:// mca-journal.org

ISSN 1859-0551

Simple balancing method for unbalanced dual-bridge converters based on fundamental harmonics approximation and trigonometric calculation

Duy-Dinh Nguyen[1*], Anh-Tan Nguyen[1], Takuya Goto[2] and Kazuto Yukita[2]

[1]*Hanoi University of Science and Technology, Vietnam*
[2]*Aichi Institute of Technology, Japan*
[*]*Corresponding author E-mail: dinh.nguyenduy@hust.edu.vn*

Abstract

Three-phase Dual-Active-Bridge converters use a three-phase transformer for isolation and voltage leveling. Due to fabrication, the inductance in the transmission path of each phase may be different from each other. If the difference is large enough, the current may be unevenly distributed among phases that lead to the unbalance in loss and heat distribution of power switches and transformers. This paper proposes a simple current balancing method among phases for three-phase Dual-Active-Bridge converters due to inductance mismatch in the transmission path. The method is based on first harmonic approximation and trigonometric calculation of the phase shift for each phase. Simulation and experimental results show that the proposed method can help balance the phase current effectively.

Keywords: *Three-phase dual-active-bridge converter; Unbalanced power distribution; Fundamental harmonics approximation; Trigonometrcs calculation; Parameters mismatch.*

Symbols

Symbols	Units	Description
L_{ka}, L_{kb}, L_{kc}	μH	total leakage inductance of phases
ψ	degrees	phase shift angle
δ_x	degrees	compensating angle
V_1, V_2	V	terminal voltages
V_{AN}, v_{an}	V	instantaneous transformer voltages
V_{AN}^f, v_{an}^f	V	fundamental component of V_{AN}, v_{an}

Abbreviations

DAB	Dual-Active-Bridge
DAB3	Three-phase Dual-Active-Bridge
V2G	Vehicle to Grid
EVSE	Electric Vehicle Supply Equipment
EV	Electric Vehicle
SPS	Single Phase Shift

Tóm tắt

Bộ biến đổi lưỡng cầu 3 pha (Dual-Active-Bridge - DAB3) sử dụng máy biến áp ba pha để cách ly và thay đổi điện áp. Do vấn đề chế tạo, thông số của điện cảm trên đường truyền tải năng lượng có thể không giống nhau giữa các pha. Nếu sự khác biệt là đủ lớn, sự mất cân bằng dòng điện giữa các pha có thể trở nên đáng kể. Hệ quả là sự phân bổ về tổn hao và phát nhiệt cũng trở nên không như nhau trên các van bán dẫn. Bài báo này đề xuất một phương pháp đơn giản để xử lý vấn đề này. Phương pháp này dựa trên việc phân tích thành phần cơ bản của dòng điện và tính toán lượng giác góc dịch pha cho từng pha. Kết quả mô phỏng và thực nghiệm cho thấy, phương pháp đề xuất có khả năng giúp cân bằng dòng điện ba pha một cách hiệu quả.

1. Introduction

In vehicle-to-grid electric vehicle supply equipment (V2G EVSE) applications, the electric power is required to flow bidirectionally between the battery and the grid. In the charging mode, the energy from the AC grid is rectified and transferred to the battery in the electric vehicle (EV). In the V2G mode, energy from the battery is inverted and injected into the grid for doing several ancillary services such as frequency or voltage regulation, load response, etc. In such applications, a bidirectional DC/DC converter system is necessary to construct the V2G EVSE.

Among various bidirectional DC/DC converter topologies, Dual-Active-Bridge (DAB) appears to be a promising choice. Firstly, it is a bidirectional topology that provides galvanic isolation capability. For applications like V2G EVSE, isolation is mandatory as listed in many technical standards. Secondly, as already discussed in many articles [1, 2], DAB topology has numerous interesting features, such as inherited soft-switching that provides noise reduction capability; high power density,

Received: 18 January 2022; Accepted: 16 March 2022.

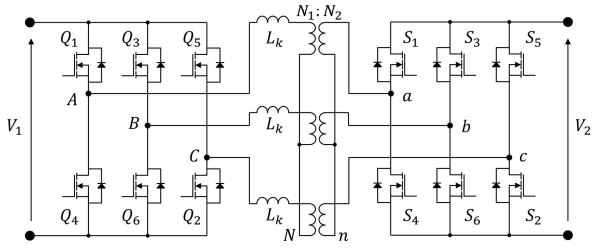

Figure 1: Three-phase dual active bridge converter topology.

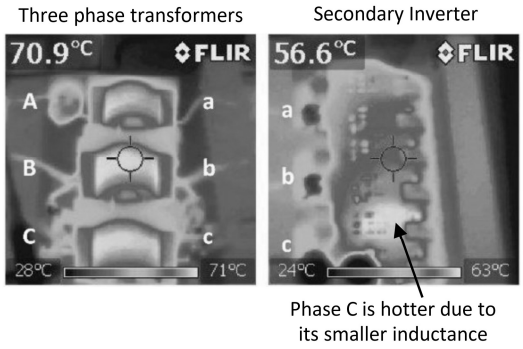

Figure 2: Thermal map at 9.3 kW of the DAB3 converter reported in [3].

and high efficiency that allow better integration, etc. For high power applications such as electric vehicle fast-charging stations, multi-phase DAB can help improve the power density even further. Figure 1 shows a three-phase DAB (DAB3) converter diagram.

The DAB3 shown in Figure 1 uses three single-phase transformers for galvanic isolation and voltage matching. The inductor L_k includes the primary-referred, total leakage inductance of the transformers and the required external series inductor (if any). For simplicity, the star-star connected transformer is considered . Two active bridges are made of two three-phase, voltage source inverters. Six-step modulation is applied for both bridges. A phase shift angle is then created between the two bridges to handle the power flow. Usually, the operation analysis of the converter is based on the assumption that the system parameters are identical for all three phases. Consequently, the power is evenly distributed among phases.

Due to many reasons such as fabrication technique, different manufactured lots, different impacts of environment on the devices, etc., system parameters may not be identical. For example, switching devices placed in different positions may suffer from unequal cooling effectiveness that leads to diverse increment of drain-source resistance of the switches; or three single-phase transformers and inductors may have different parameters due to the winding technique or nonidentical magnetic material that yields to the dissimilarity of the equivalent series inductance, etc. In fact, in DAB-based topologies, L_k plays an essential role in power transferring because it acts as the energy container in the transmission. A slight difference in the equivalent series inductance among three phases may lead to serious problems.

For instance, in [3], L_k was integrated into the transformers. Integration is a good idea to downsize the converter, reduce the production cost, and increase system reliability [4, 5]. However, the integration depends a lot on the winding technique of the transformers. As reported in [3], there was only 2% difference at most in the values of L_k among phases. From a practical view, 2% deviation in the leakage inductance is acceptable when considering the tolerance of commercial power inductors which is usually ranging from 10% to 15% [6]. However, the thermal map captured by a thermal camera given in [3] (Figure 2) showed that phase C that owns the smallest leakage inductance seems to be the hottest one among three phases. This implies that the power dissipation in phase C is greater than that of the other two phases. As a consequence, a hot spot is formed and the risk of over-heat is higher and sooner than normal. Besides, the overall efficacy may be reduced. Therefore, it is necessary to balance the loss distribution among phases when parameters mismatching occurs.

Various balancing techniques for multi-phase DC/DC converter can be found in the literature. Closed-loop control based techniques [7, 8, 9] are usually applied for multi-phase buck/boost converter where average current mode control is employed for each phase, therefore, the current flowing in each phase is always identical owing to the current regulation regardless of the parameter mismatch. This approach is a good choice for topologies where the imbalance current is DC. However, for isolated DC/DC converter topologies like DAB3, multi-phase LLC DC/DC, etc., the imbalanced current is pure AC, therefore, it is difficult to apply such the methods.

Another approach was presented in [10] for multi-modular isolated DC/DC resonant converters. Accordingly, an coupling transformer was added to link the two modules aiming to balance the current between them. The additional transformer was then integrated with the resonant inductors into a single magnetic device to save space. However, this introduces further effort on hardware redesign. Besides, this approach is difficult to apply to the case of DAB3 converters. Similarly, in [11], the transformer of a three-phase LLC DC/DC converter was redesigned for balancing purpose. However, the special shaping and designing technique of the transformer can increase cost and complexity of production. Besides, only the magnetic core was optimized for balancing purpose, the winding technique which strongly affects the leakage inductance parameters was not discussed in the study.

Some other researches do not redesign the hardware but modify the control strategy to improve the unbalance current problem. In [12], the current sharing for an unbalanced three-phase LLC resonant converter was undertaken by modifying the inner phase shift among three phases. The inner phase shift was calculated based on the root-mean-square values of phase currents; hence, this method required the phase current to be measured. Using feedback control to deal with the unbalance may be a good approach from the viewpoint of effectiveness. However, considering the high operating frequency of the converter ($\sim$200 kHz), sampling and processing the transformer current may add burdens to the overall control system. In [13], the imbalance of current of a DAB3 converter was resolved by applying different phase shift for each phase of a DAB3. However, the calculation of the phase shift was not presented clearly in the article. Some other techniques are introduced for DAB3 to solve the unbalance current problems [14, 15], however, similar to [13], these studies only dealt with the transient unbalance caused by pulsating load changes. Studies on applying those techniques to balance the current in a DAB3 with mismatched parameters are hardly to be found in the literature.

In this paper, a simple method is introduced to balance the phase current when there is mismatching in transferring inductance in the transmission paths. The approach is similar to that reported in [13] which uses modified phase shift angles for each phase of the converter to balance the current unbalance due to parameters mismatching. The proposed method is based on the first harmonics analysis of the transmission power when single phase shift (SPS) modulation control which mimics the approach presented in [12] is employed. Then, the proposed open-loop balancing rule is derived using trigonometric calculations. The rest of this paper is structured as follows: operation principle of the converter under SPS is given in Section 2; analysis and derivation of formula to determine the phase shift are provided in Section 3; finally, simulation results presented in Section 4 will confirm the proposed technique.

2. Three-phase Dual-Active-Bridge converter

Three-phase Dual-Active-Bridge (DAB3) converters is a member of the DAB converter family which contains two active bridges and an isolated transformer. Figure 1 illustrates the simplified diagram of the converter. Two three-phase inverters are located at the primary and secondary sides of a three-phase transformer. For high power applications, the inverters are usually built up by Silicon-Carbide Metal-Oxide-Semiconductor Field-Effect Transistor (SiC-MOSFETs), whereas the three-phase transformer is usually formed by three single-phase transformers aiming to simplify the production process. For simplicity, the transformer with the star-star connection is assumed.

Conventionally, the SPS modulation is employed to handle the power flow in the converter. Ideally, the duty cycle of each switch is 50% in complementary mode, and each phases is 120 degrees shifted from each other. Accordingly, two three-phase square wave voltages are created at the two sides of the transformer. A phase shift angle of ψ degrees between the two bridges is then used to shift the secondary voltage back or forth with regard to the primary voltage, and hence, handling the power transmission. Figure 3 shows the simplified diagram of the DAB3 converter. Notes that, all the voltages shown in the diagram are referred to the neutral point of the transformer. In this figure, L_{kx} is the total primary-referred inductance (including the external series inductor, if any) of the transformer in the corresponding phase where $x \in [a,b,c]$. Figure 4 illustrates the theoretical phase voltage and current waveform obtained by using the SPS modulation technique.

Let us make some assumptions:

- the system parameters are identical among phases (i.e. $L_{ka} = L_{kb} = L_{kc} = L_k$),
- the power is evenly distributed,
- and the power loss is ignored,

according to [3], the total power transmission through the transformer can be calculated by:

$$P = \frac{nV_1V_2}{12f_sL_k}\psi\left(4 - \frac{3\psi}{\pi}\right) \tag{1}$$

where L_k is the total primary-referred leakage inductance of the transformer; f_s is the switching frequency; V_1 and V_2 are the terminal DC voltages; and n is the transformer winding ratio. Equation (1) is obtained by multiplying the output current and

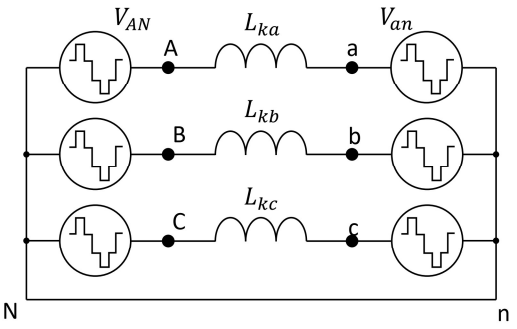

Figure 3: Simplified diagram of the DAB3 converter.

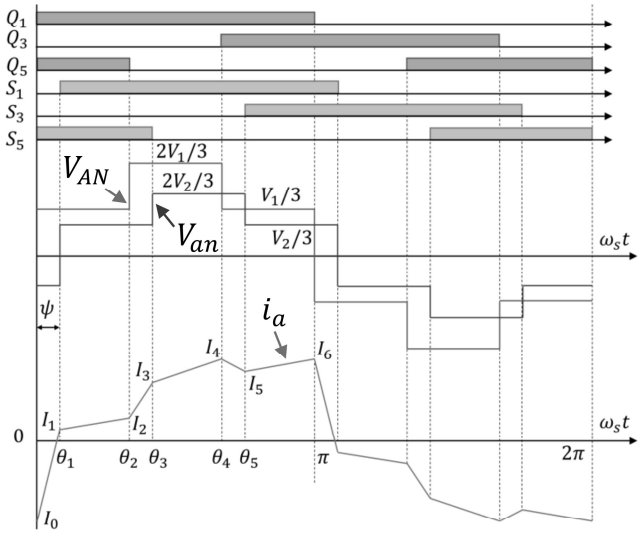

Figure 4: Theoretical voltage and current waveform by SPS modulation.

the output voltage at the steady state. The calculation of the output current is undertaken by solving the transition currents at each switching state. This calculation is simple and feasible when all the phase parameters are identical. However, when there is a parameter mismatch, solving equations for transition currents become complicated.

Now, considers the fundamental component of the voltages across the primary and secondary sides of, for example, phase A transformer. The phase voltages have a four-level form, and their primary-referred fundamental component can be expressed by:

$$v_{AN}^f(t) = \frac{2V_1}{\pi}\sin(2\pi f_s t) \tag{2}$$

$$v_{an}^f(t) = \frac{2nV_2}{\pi}\sin(2\pi f_s t - \psi) \tag{3}$$

The superscript ^{f} implies the fundamental component of the corresponding quantity. The transmission power between the two sinusoidal systems having a phase displacement of ψ is:

$$P_a^f = \frac{\left\|V_{AN}^f\right\| \cdot \left\|V_{an}^f\right\|}{2X_a}\sin\psi \tag{4}$$

where X is the reactance between the two sinusoidal systems, here $X_a = 2\pi f_s L_{ka}$; $\left\|V_{AN}^f\right\|$ and $\left\|V_{an}^f\right\|$ are the modulus of the fundamental components of primary and secondary voltages of phase A, $\left\|V_{AN}^f\right\| = \frac{2V_1}{\pi}$ and $\left\|V_{an}^f\right\| = \frac{2nV_2}{\pi}$. Substituting into (4),

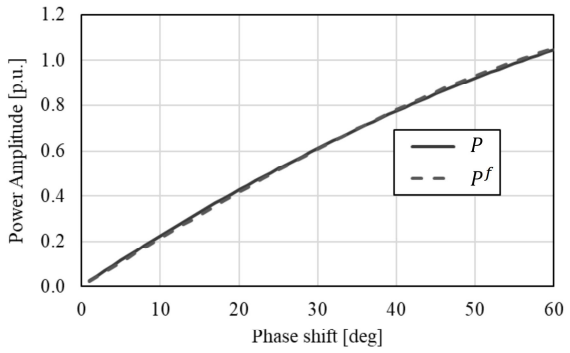

Figure 5: Power versus phase shift characteristics.

the power transferred by the fundamental component through phase A is:

$$P_a^f = \frac{2nV_1V_2}{\pi^2 X_a}\sin\psi \tag{5}$$

If three-phase reactance is identical, the total fundamental power transmission is calculated by:

$$P^f = \frac{6nV_1V_2}{\pi^2 X_a}\sin\psi \tag{6}$$

Figure 5 illustrates the comparison between P and P_f versus phase shift angle ψ in the range from 0 degrees to 60 degrees. In this figure, the continuous line denotes the power transmission determined by (1), whereas the dashed line shows the power transferred by only the fundamental component according to (6). As shown, there are mostly no differences between the two power characteristics. While the derivation of P depends strongly on the transition currents which are determined by solving some highly parameter-dependent equations, the yielding of P_a^f is relatively independent of phase B and C parameters. Therefore, in the upcoming analysis, P_x^f with $x \in [a,b,c]$ is employed to investigate the power distribution in the occurrence of parameter mismatching problem.

3. Power balancing method

Analysis in the last section assumed an identical reactance of three phases. However, due to many reasons, such as winding technique, magnetic material performance variation, etc., the reactance may be different. As a consequence, for the same phase shift angle ψ, the phase owning the smallest reactance will have the highest power flow, and vice versa. Therefore, in order to balance the power among phases, different phase shift angles are used for different phases. Let ψ_a, ψ_b and ψ_c are the actual phase shift angles of the corresponding phases, from (5), the fundamental power in each phase can be expressed by:

$$\begin{cases} P_a^f = \dfrac{2nV_1V_2}{\pi^2 X_a}\sin\psi_a \\ P_b^f = \dfrac{2nV_1V_2}{\pi^2 X_b}\sin\psi_b \\ P_c^f = \dfrac{2nV_1V_2}{\pi^2 X_c}\sin\psi_c \end{cases} \tag{7}$$

Notably, in DAB3 converter control systems, there is usually only one current controller to regulate the current at the receiving side. The output of the controller is the bridge phase shift ψ. Therefore, it is more convenient to derive ψ_a, ψ_b and ψ_c from ψ as:

$$\psi_x = \psi + \delta_x, \forall x \in [a,b,c] \tag{8}$$

where δ_x is the phase deviation of ψ_x compared to ψ. It is also the compensating phase angle that the controller must provide to compensate for the parameter mismatch. If δ_x is small enough, $\sin\psi_x$ can be approximated by:

$$\begin{aligned} \sin\psi_x &= \sin(\psi+\delta_x) \\ &\approx \sin\psi + \delta_x\cos\psi \end{aligned} \tag{9}$$

Substituting (9) into (7), we have:

$$\begin{cases} P_a^f \approx \dfrac{2nV_1V_2}{\pi^2}\cdot\dfrac{\sin\psi+\delta_a\cos\psi}{X_a} \\ P_b^f \approx \dfrac{2nV_1V_2}{\pi^2}\cdot\dfrac{\sin\psi+\delta_b\cos\psi}{X_b} \\ P_c^f \approx \dfrac{2nV_1V_2}{\pi^2}\cdot\dfrac{\sin\psi+\delta_c\cos\psi}{X_c} \end{cases} \tag{10}$$

Aiming for power to be evenly distributed among phases, the phase deviation δ_x is designed so that:

$$\frac{\sin\psi+\delta_a\cos\psi}{X_a} = \frac{\sin\psi+\delta_b\cos\psi}{X_b} = \frac{\sin\psi+\delta_c\cos\psi}{X_c} = \frac{\sin\psi}{\langle X\rangle} \tag{11}$$

where $\langle X\rangle$ is the average reactance, determined by:

$$\langle X\rangle = \frac{X_a+X_b+X_c}{3}.$$

Solving (11) for δ_x, we have:

$$\begin{cases} \delta_a = \dfrac{X_a-\langle X\rangle}{\langle X\rangle}\tan\psi \\ \delta_b = \dfrac{X_b-\langle X\rangle}{\langle X\rangle}\tan\psi \\ \delta_c = \dfrac{X_c-\langle X\rangle}{\langle X\rangle}\tan\psi \end{cases} \tag{12}$$

Values of δ_x determined by (12) depends on how large X_x is deviated from $\langle X\rangle$ and how big the common bridge phase shift

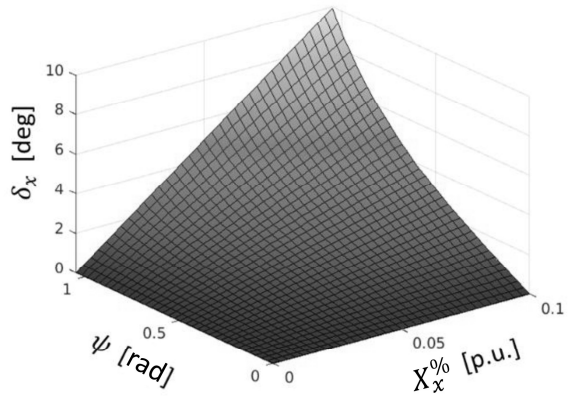

Figure 6: Dependence of δ_x versus reactance deviation and bridge phase shift.

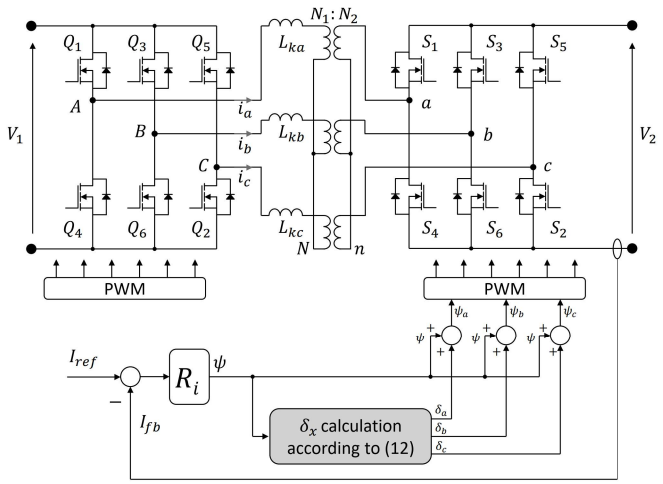

Figure 7: Current control loop diagram with the proposed power balancing technique.

ψ is. That dependency is demonstrated in Figure 6. In the figure, $X_x^{\%}$ is the relative deviation of X_x from $\langle X \rangle$,

$$X_x^{\%} = \frac{X_a - \langle X \rangle}{\langle X \rangle}.$$

It is easy to observe that the phase shift deviation δ_x is directly proportional to the relative reactance deviation. When the relative reactive deviation is 10% and the bridge phase shift ψ is 60 degrees, the phase deviation of the corresponding phase is as large as 10 degrees. In this case, the assumption of small signal δ_x is not violated as the approximation error is insignificant:

$$\frac{\sin(\psi + \delta_x)}{\sin\psi + \delta_x \cos\psi} = \frac{0.94}{0.95} \approx 98.95\%$$

Even when the relative reactance deviation is 20%, and the phase shift is 60 degrees, the aforementioned assumption is still acceptable as the error is around 5%:

$$\frac{\sin(\psi + \delta_x)}{\sin\psi + \delta_x \cos\psi} = \frac{0.98}{1.04} \approx 94.23\%$$

Of course, the approximation error will be smaller when the reactance deviation and/or the control phase shift are small. In fact, in order to limit the reactive power transferring through the transformer, the control phase shift angle is usually designed in the range from -30 degrees to +30 degrees. Therefore, the approximation error by (9) can be ignored, and rule (12) can be employed to compensate for the mismatching of reactance in the transmission path.

Figure 7 demonstrates the implementation of the current control loop together with the proposed power balancing technique. The proposed technique is implemented as a post-processing processing procedure after a new phase shift angle is calculated by the current controller. According to (12), the relative reactance deviation can be calculated in advance, therefore, only $\tan\psi$ must be computed in the run-time. By the utilization of a floating-point processing unit, or CORDIC algorithm, or look-up table technique, the tangent function can easily be calculated just in several CPU cycles [16].

4. Results and Discussion

Aiming to demonstrate the effectiveness of the proposed balancing technique, simulation study is conducted. The inductance is made different from each other intentionally. Simulation is carried out under several conditions of deviation and operation conditions. Parameters of the simulating system are summarized in Table 1. In this simulation study, the total leakage inductance of phases A, B, and C are intentionally made different from the designed value. In particular, there are three investigated cases as follows:

Table 1: System parameters.

Parameter	Symbol	Value	Unit
Input voltage	V_1	400	V
Output voltage	V_2	320∼420	V
Transformer ratio	n	1:1	
Total leakage inductance (expected)	L_k	5	μH
Reactance deviation	$X_x^{\%}$	10 ∼ 30%	
Switching frequency	f_s	100	kHz
Phase shift angle	ψ	0∼ 30	degrees

4.1. Case study 1: $L_{ka} = 5$ μH, $L_{kb} = L_{kc} = 6.5$ μH

In this case study, the phase A leakage inductance is assumed to be as good as designed, however, phases B and C have the same inductance and are 30% greater than that of phase A. The average leakage inductance is thus 6 μH. The deviation of inductance in each phase compared to the average one is 20%, 8.3%, and 8.3%, respectively. In practice, this case study is likely to occur where one phase owns a leakage inductance that is significantly smaller than the other two phases, although the deviation may be not as large as being considered.

Figure 8(a) shows the phase current waveform when the phase shift is 30 degrees for all three phases and the voltage conversion ratio is 1:1. As expected, phase A current is the largest among three phases. Its peak current is 10 amperes (or 13.7%) greater than that of phases B and C. The root-mean-squared (RMS) of the three phases are 55.1, 49.3, and 49.1 amperes, respectively. If the switches have same ON resistance, this current deviation causes about 25% more dissipation on phase A than phases B and C.

The difference in phase currents is remarkably reduced by applying the proposed balancing technique, as shown in Figure 8(b). Phase A current remains the largest one among three phases, however, the gap to other phases reduces to only 3.9 amperes, which is about 2.56 times smaller than the latter case. In terms of RMS current, the difference is even smaller. The RMS current of phases A, B, and C are 50.2, 51.9, and 50.1 amperes for each phase, respectively, which means the most lossy phase dissipates only 7.3% more than the other two phases (assuming switching devices owning same ON resistance). Compared to the latter case, the loss is reduced significantly by 3.4 times.

Figure 9 illustrates the effect of the proposed balancing technique on RMS currents under various cases of phase shift angles. As seen in Figure 9(a), phase B and C RMS currents are mostly same because their inductances are identical, whereas, phase A RMS current is the largest one in all cases of phase shift angles. When the proposed balancing method is applied, the difference in RMS currents among phases is expressively reduced as shown in Figure 9(b). When the phase shift is smaller than 20 degrees, the three phase RMS currents can be considered as equal. When ψ is greater than or equal to 20

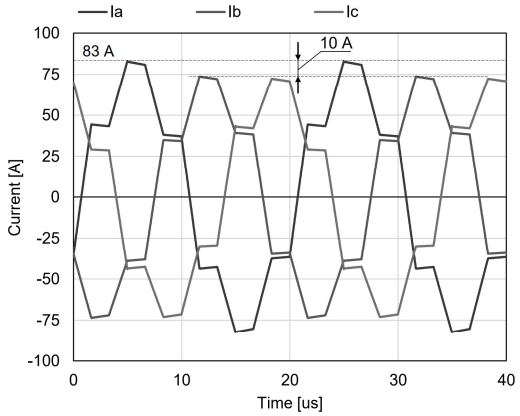

(a)

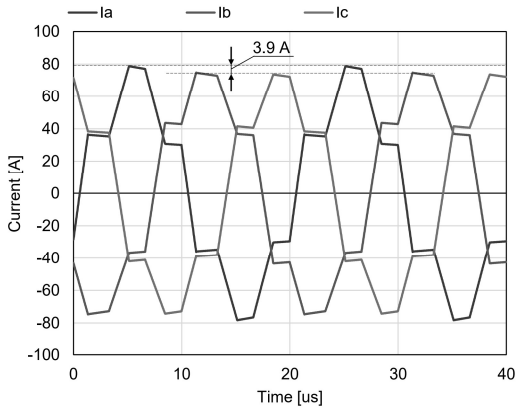

(b)

Figure 8: Phase current in Case study 1 when $\psi = 30$ degrees: (a) under the original SPS modulation; (b) when the proposed balancing technique is applied.

degrees, the distinction between phase RMS currents is less than 3.6%. Therefore, it can be concluded that, the proposed balancing technique is effective in the case where one phase has significantly smaller inductance than other phases.

4.2. Case study 2: $L_{ka} = L_{kb} = 5$ μH, $L_{kc} = 6.8$ μH

In this case study, the phase A and B leakage inductances are assumed to be 5μH as designed, however, phase C has a notably larger inductance of 6.8 μH. The average inductance is 5.6 μH, and thus, the deviation compared to the average one is 10.7%, 10.7%, and 21.4%, respectively. In practice, this case study is also likely to occur where one phase owns a significantly larger leakage inductance than the other two phases, although the deviation may be not as large as being considered.

Figure 10 depicts the effect of the proposed balancing technique on RMS currents in this case study. As expected, when the original SPS modulation is employed, phase C which owns the largest leakage inductance exhibits the smallest RMS current compared to other phases as seen in Figure 10(a). In particular, when the phase shift is 30 degrees, phase B RMS current is 18.7% greater than that of phase C, and the distinction is 9.2 amperes. When the proposed balancing technique is applied, the RMS current deviation is greatly reduced as shown in Figure 10(b). The biggest current difference of 3.6 amps (equivalent to 6.9%) is observed when the phase shift is 30 degrees. In other words, the current unbalance is suppressed by about three times compared to that before applying the proposed method. Therefore, in this case study also, it can be concluded that the proposed technique is effective in dealing with the current unbalance due to the inductance mismatch.

4.3. Case study 3: $L_{ka} = 4.0$ μH, $L_{kb} = 5.0$ μH, $L_{kc} = 6.0$ μH

In this case study, the leakage inductances are assumed to be 4μH, 5μH, and 6μH, respectively. The average inductance is 5.0μH, and thus, the deviation compared to the average one is 20%, 0%, and 20%, respectively. In practice, this case study is unlikely to occur because the assembling engineers usually tend to pick components having similar parameters as much as possible. However, it is worth having this case investigated as the "worst" case to demonstrate the effect of the proposed balancing technique.

Figure 11 exhibits the phase RMS currents in various cases of phase shift angles with and without the proposed balancing method applied. As expected, when the original SPS modulation is used, phase A which owns the smallest leakage inductance has the highest RMS current, whereas, phase C that owns the largest inductance has the smallest RMS current as seen in Figure 11(a). In particular, when the phase shift is 30 degrees, phase A RMS current is 67.6 amperes which is 11.8 amperes (equivalent to 21.1%) greater than that of phase C. When the proposed method is applied, the RMS currents are greatly balanced as shown in Figure 11(b). The largest current difference is only 4.1 amps (equivalent to 6.95%) observed at the phase shift of 30 degrees. Compared to that without the proposed method, the current unbalance is three times reduced. Therefore, in this "worst" case study either, the same conclusion as the two latter cases can also be made.

4.4. Discussion

In summary, from the three investigated cases above, the proposed balancing technique can help to reduce the RMS current unbalance effectively in the cases where one phase has notably greater/smaller inductance than the others, or even the case where three inductance are greatly different from each other. In all cases, the unbalance is reduced by around 3 times at most when the reactance deviation is as large as 20%. Although bringing significant benefit, the method uses only some simple calculations that can be accomplished just in several tens of CPU cycles. In addition, no extra sensors or measurements are required to provide further information to the calculation in the run-time. With this little effort, the conduction loss can be better distributed among phases without adding extra cost or burden to the whole control system.

However, the proposed balancing technique required the total leakage inductance parameters of all phases to calculate the compensating phase angle. If the inductance is falsely measured or drifted, or changed during run-time, the effects of the proposed technique will be reduced. Besides, this technique could be feasible to microprocessors supporting floating-point or fixed-point units. For the lower specs processors, a look-up table might be used to compute the trigonometric functions.

Besides, the proposed method is based on the fundamental harmonics. Although the analysis shows a good matching between the transferred power computing by the fundamental and the actual components, there is still mismatch between them. Besides, the calculation ignores the core loss of the transformers,

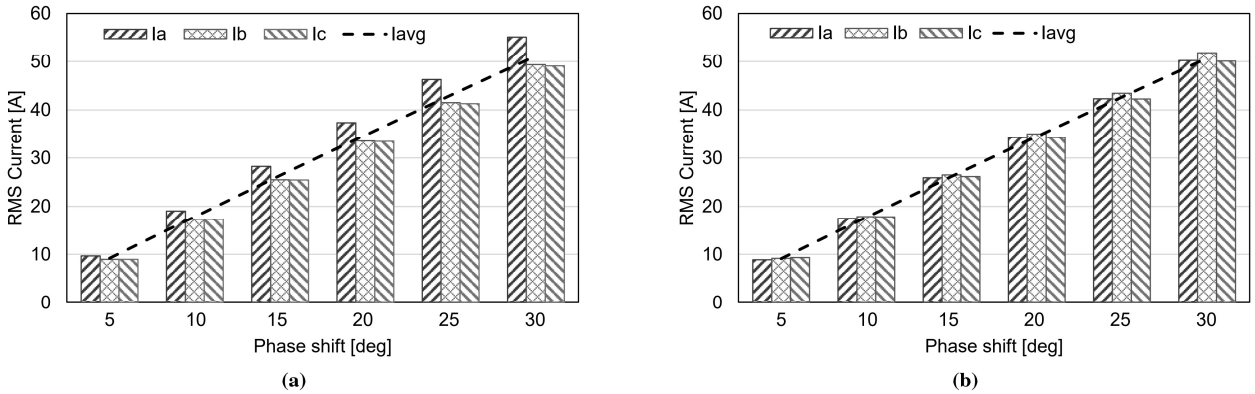

Figure 9: Phase RMS current in Case study 1 with different phase shift angle: (a) under the original SPS modulation; (b) when the proposed balancing technique is applied.

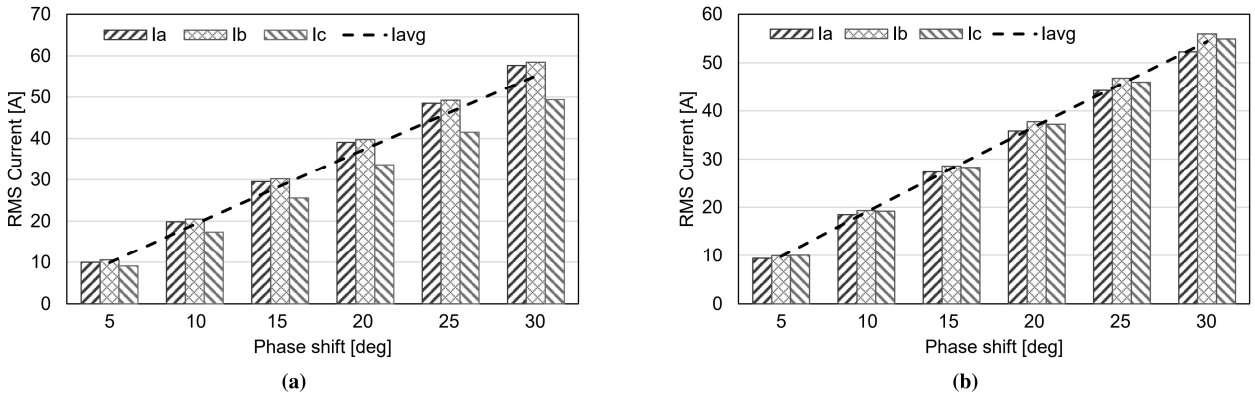

Figure 10: Phase RMS current in Case study 2 with different phase shift angle: (a) under the original SPS modulation; (b) when the proposed balancing technique is applied.

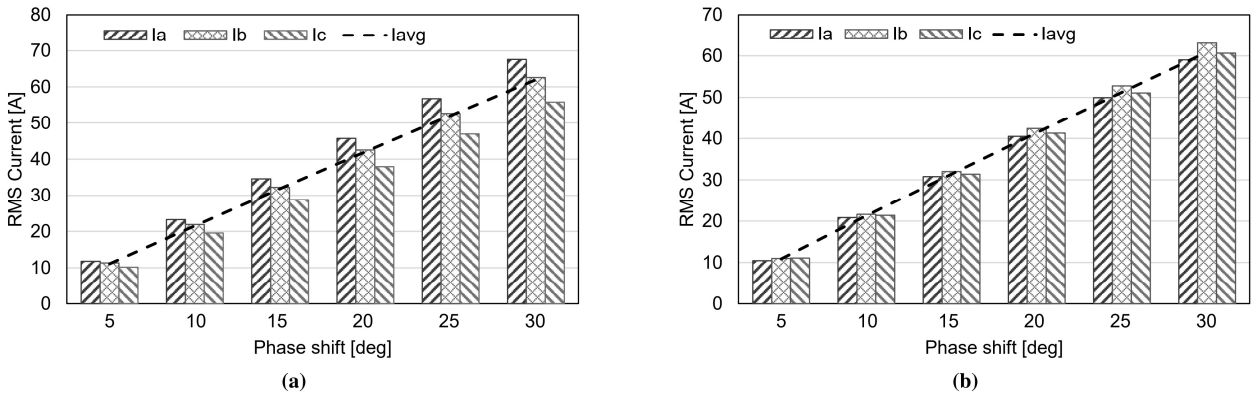

Figure 11: Phase RMS current in Case study 3 with different phase shift angle: (a) under the original SPS modulation; (b) when the proposed balancing technique is applied.

and the switching loss is also not taken into account. In the future works of this study, those factors will be addressed and trade-off with the computation burden.

5. Conclusion

This paper proposes a power balancing technique base on the fundamental harmonics approximation of the power transfer for three-phase DAB converters that have nonidentical inductance in the transmission paths. The approach is to compensate for the parameter mismatch by adding an appropriate deviation angle into the phase shift of each phase. The calculation of compensating angles is simple and feasible to deploy in mid-range micro-processors. Simulation results show that, the proposed technique is effective in reducing the unbalance by three times, owing to that, the power is better distributed among phases, and the overall system performance could be enhanced.

Acknowledgement

This research is funded by Hanoi University of Science and Technology (HUST) under project numbered T2021-SAHEP-005.

References

[1] B. Zhao, Q. Song, W. Liu, and Y. Sun, "Overview of dual-active-bridge isolated bidirectional dc–dc converter for high-frequency-link power-conversion system," *IEEE Trans. Power. Electron.*, vol. 29, no. 8, pp. 4091–4106, 2014.

[2] X. She, A. Q. Huang, and R. Burgos, "Review of solid-state transformer technologies and their application in power distribution systems," *IEEE Journal of Emerging and Selected Topics in Power Electronics*, vol. 1, no. 3, pp. 186–198, 2013.

[3] D.-D. Nguyen, K. Yukita, A. Katou, and S. Yoshida, "Design optimization of a three-phase dual-active-bridge converter for charging stations," in *2019 IEEE Vehicle Power and Propulsion Conference (VPPC)*. IEEE, 2019, p. in process.

[4] M. Mu, L. Xue, D. Boroyevich, B. Hughes, and P. Mattavelli, "Design of integrated transformer and inductor for high frequency dual active bridge gan charger for phev," in *2015 ieee applied Power electronics conference and exposition (aPec)*. IEEE, 2015, pp. 579–585.

[5] Y. Park, S. Chakraborty, and A. Khaligh, "Dab converter for ev on-board chargers using bare-die sic mosfets and leakage-integrated planar transformer," *IEEE Transactions on Transportation Electrification*, 2021.

[6] "Product tolerance guide," https://www.micrometals.com/products/product-tolerance-guide/, accessed: 2022-01-13.

[7] H.-C. Chen, C.-Y. Lu, and U. S. Rout, "Decoupled master-slave current balancing control for three-phase interleaved boost converters," *IEEE Transactions on Power Electronics*, vol. 33, no. 5, pp. 3683–3687, 2017.

[8] S. Angkititrakul, H. Hu, and Z. Liang, "Active inductor current balancing for interleaving multi-phase buck-boost converter," in *2009 Twenty-Fourth Annual IEEE Applied Power Electronics Conference and Exposition*. IEEE, 2009, pp. 527–532.

[9] K.-I. Hwu and Y. Chen, "Current sharing control strategy based on phase link," *IEEE Transactions on Industrial Electronics*, vol. 59, no. 2, pp. 701–713, 2011.

[10] U. Ahmad, H. Cha, and N. Naseem, "Integrated current balancing transformer based input-parallel output-parallel llc resonant converter modules," *IEEE Transactions on Power Electronics*, vol. 36, no. 5, pp. 5278–5289, 2020.

[11] M. Noah, S. Endo, H. Ishibashi, K. Nanamori, J. Imaoka, K. Umetani, and M. Yamamoto, "A current sharing method utilizing single balancing transformer for a multiphase llc resonant converter with integrated magnetics," *IEEE Journal of Emerging and Selected Topics in Power Electronics*, vol. 6, no. 2, pp. 977–992, 2017.

[12] S. A. Arshadi, M. Ordonez, W. Eberle, M. A. Saket, M. Craciun, and C. Botting, "Unbalanced three-phase *llc* resonant converters: Analysis and trigonometric current balancing," *IEEE Transactions on Power Electronics*, vol. 34, no. 3, pp. 2025–2038, 2018.

[13] S. P. Engel, N. Soltau, H. Stagge, and R. W. De Doncker, "Dynamic and balanced control of three-phase high-power dual-active bridge dc–dc converters in dc-grid applications," *IEEE Trans. Power. Electron.*, vol. 28, no. 4, pp. 1880–1889, 2013.

[14] J. Huang, Z. Li, L. Shi, Y. Wang, and J. Zhu, "Optimized modulation and dynamic control of a three-phase dual active bridge converter with variable duty cycles," *IEEE Transactions on Power Electronics*, vol. 34, no. 3, pp. 2856–2873, 2018.

[15] J. IIu, S. Cui, S. Wang, and R. W. De Doncker, "Instantaneous flux and current control for a three-phase dual-active bridge dc–dc converter," *IEEE Transactions on Power Electronics*, vol. 35, no. 2, pp. 2184–2195, 2019.

[16] STMicroelectronics, "Getting started with the cordic accelerator using stm32cubeg4 mcu package," Tech. Rep., 2021.